Toxicology Letters 238 (2015) 7–16

Contents lists available at ScienceDirect

Toxicology Letters

journal homepage: www.elsevier.com/locate/toxlet

P9a(*Cdt*-PLA$_2$) from *Crotalus durissus terrificus* as good immunogen to be employed in the production of crotalic anti-PLA$_2$ IgG

Luciano S. Fusco[a,c], Juan Pablo Rodríguez[a,*], Frank Torres-Huaco[b], Salomón Huancahuire-Vega[b], Pamela Teibler[c], Ofelia Acosta[c], Sergio Marangoni[b], Luis Alberto Ponce-Soto[b], Laura C. Leiva[a]

[a] Protein Research Laboratory (LabInPro), Faculty of Natural Sciences and Surveying (FACENA), National Northeastern University (UNNE), Corrientes 3400, Argentina
[b] Department of Biochemistry, Institute of Biology (IB), State University of Campinas (UNICAMP), Campinas, SP, Brazil
[c] Laboratory of Pharmacology, Faculty of Veterinary Science, National Northeastern University (UNNE), Argentina

HIGHLIGHTS

- We propose the use of a PLA$_2$ isoform from *C.d.t.* venom to be used as immunogen.
- P9a(*Cdt*-PLA$_2$) has the lowest toxicological activity among the isoforms from the venom.
- P9a(*Cdt*-PLA$_2$) IgG antibodies can be easily produced in laboratory animals.
- P9a(*Cdt*-PLA$_2$) IgG antibodies can cross react with the other isoforms from the venom.

ARTICLE INFO

Article history:
Received 2 January 2015
Received in revised form 18 June 2015
Accepted 22 June 2015
Available online 27 June 2015

Keywords:
Snake venom
Rattlesnake
HPLC-PR
Myotoxin
Neurotoxicity
Antivenom

ABSTRACT

Four proteins with phospholipase A$_2$ (PLA$_2$) activity, designated P9a(*Cdt*-PLA$_2$), P9b(*Cdt*-PLA$_2$), P10a(*Cdt*-PLA$_2$) and P10b(*Cdt*-PLA$_2$) were purified from the venom of *Crotalus durissus terrificus* by two chromatographic steps: a gel filtration and reversed phase HPLC. The profile obtained clearly shows that three of them have a similar abundance. The molecular mass, 14193.8340 Da for P9a(*Cdt*-PLA$_2$), 14134.9102 Da for P9b(*Cdt*-PLA$_2$), 14242.6289 Da for P10a(*Cdt*-PLA$_2$) and 14183.8730 Da for P10b(*Cdt*-PLA$_2$), were initially evaluated by SDS-PAGE and confirmed by ESI-Q-TOF spectrometry, and all of them displayed a monomeric conformation. Also, partial amino acid sequence of each protein was obtained and their alignments with other crotalic PLA$_2$ revealed a high degree of identity among them. Additionally, we studied some pharmacological activities like neurotoxicity, myotoxicity and lethality, which prompted us to pick two of them, P9a(*Cdt*-PLA$_2$) and P10a(*Cdt*-PLA$_2$) that resulted to be less toxic that the others, and further characterize them to be used as immunogen. We next injected these last proteins in mice to produce antitoxins against them and ELISA and dot blots reveled that both toxins do not show immunogenic differences, unlike those other pharmacologic activities tested. Furthermore, the antibodies produced cross-reacted with all the isoforms purified demonstrating the feasibility of using only one of them and ensuring the cross-reaction of all.

The results obtained show that P9a(*Cdt*-PLA$_2$) isoform has the lowest toxicity and also a good purification performance; thus this protein may be a promising candidate to be employed in the production of crotalic antitoxins.

1. Introduction

Crotoxin, the major lethal toxin of South American rattlesnake (*Crotalus durissus terrificus, C.d.t.*) venom, was the first snake venom protein to be purified and crystallized (Gutierrez, 2002). Crotoxin is a heterodimeric β-neurotoxin that consists of a toxic

* Corresponding author.

http://dx.doi.org/10.1016/j.toxlet.2015.06.528
0378-4274/

basic phospholipase A_2 (PLA_2) and a nonenzymatic, non-toxic acidic component (crotapotin) (Hendon and Fraenkel-Conrat, 1971). Crotoxin blocks the neuromuscular transmission; it acts primarily at the presynaptic level of neuromuscular junctions by impairing neurotransmitter release. Additionally, other biological activities normally attributed to crotoxin include myotoxicity, nephrotoxicity and cardiotoxicity. On the other hand, in recent years, there has been increasing evidence that crotoxin exerts a variety of other important actions unrelated to these activities. These actions include immunomodulatory, anti-inflammatory, antitumor, anti-microbial and analgesic activities (Sampaio et al., 2010).

Crotoxin PLA_2 subunit belong to an expanding superfamily of enzymes, which catalyzes hydrolysis of the ester bond at the *sn-2* position of 1,2-diacyl-*sn*-3-phosphoglycerides, generating lysophospholipids and free fatty acids (Kini, 2003). Crotalic PLA_2 displays similar pharmacological effects to those exhibited by crotoxin, however, in the case of lethality, higher doses of PLA_2 are required. Because of that, it is believed that crotapotin behaves as a carrier for the PLA_2, reducing its non-specific interaction, therefore, increasing the binding with its target and enhancing the toxicity of crotoxin (Hendon and Fraenkel-Conrat, 1971, 1976; Hendon and Tu, 1979). Additionally, since PLA_2 shows less toxicity than the whole venom, its use as immunogen has been proposed in order to obtain antitoxins to be use in crotalic envenomations (Fusco et al., 2014; Rodríguez et al., 2006).

Crotoxin has been shown to be a mixture of isoforms present in the whole venom. They result from combinations of several variants of each subunit. Purified PLA_2 isoforms consist of a single polypeptide chain of 121/2 amino acids, differing from each other by only few amino acids as determined by amino-acid composition (Faure et al., 1994). These differences create diversity in their biological functions, allowing the existence of an isoform among them that can be obtained with acceptable purity, would have low toxicity and good immunogenic capacity. Thus, this protein could be useful in the production of antitoxins.

PLA_2s from *C.d.t.* venom were isolated and sequenced from Brazilian specimens by several authors (Damico et al., 2005; Marchi-Salvador et al., 2007; Ponce-Soto et al., 2006, 2007a; Romero-Vargas et al., 2010; Toyama et al., 2000), however most of these studies have been limited to an exhaustive biochemical characterization, and none of them focuses on their potential use as immunogens.

There is no available information about PLA_2 sequences isolated from *C.d.t.* venom from Argentina and considering regional variations not only among species, but also within a single species, this represents an exceptional reservoir to explore and find useful alternatives to be employed in technological applications (Fernandez et al., 2010; Saravia et al., 2002). Thus, to address this challenge a comprehensive understanding of the sequences-structure-biological function relationship result essential.

In this work, we describe the biochemical, pharmacological and immunological characterization of PLA_2 isoforms, isolated from *C. d.t.* snake venom, in order to provide evidence for selecting the best candidates to be employed in the production of crotalic anti-PLA_2 IgG.

2. Material and methods

2.1. Venom and animals

C.d.t. venom was pooled from 10 specimens of 8/10-year-old adult snakes held in the serpentarium of the local Zoo, Corrientes, Argentina. The venom was lyophilized and kept frozen at −20 °C. Male Swiss white mice weighing 20–22 g were supplied by the Animal Services Unit of the State University of Campinas (UNICAMP). The mice were housed at 25 °C on a 12 h light/dark cycle. Male young chickens (4–8 days old, HY-LINE W36 lineage) were supplied by Granja Ito S/A (Campinas, SP, Brazil). All animals had free access to food and water and were conducted in accordance with guidelines of the Ethics Committee of the Biology Institute-UNICAMP (Campinas, Brazil).

2.2. Toxins purification

2.2.1. Molecular exclusion chromatography

Venom (25 mg) was dissolved in 50 mM ammonium bicarbonate (pH 8.0), and fractionated on a Sephadex G75 column (1 × 75 cm), eluted with the same buffer at a constant flow of 0.5 ml/min. Elution was monitored at 280 nm, and the fractions were immediately lyophilized and stored at −20 °C.

2.2.2. Reverse phase (RP) HPLC

Four mg of the fraction obtained from Sephadex G75 (Peak II) were dissolved in 200 μl of solvent A (0.1% (v/v) trifluoroacetic acid; TFA). The resulting solution was clarified by centrifugation and the supernatant was applied to a μ-Bondapack C18 column (0.78 × 30 cm; Waters 991-PDA system). Proteins were eluted with a gradient (0–20%, 20–60%, 60–100%) of 66% (v/v) acetonitrile in solvent B, at a flow rate of 1 ml/min. The elution profile was monitored at 280 nm and the fractions were collected, lyophilized and stored at −20 °C.

2.3. Molecular mass determination and protein sequencing

2.3.1. Molecular mass determination

An aliquot (4.5 μl) of the purified protein was injected by C18 (100 μm × 100 mm) RP-UPLC (nanoAcquity UPLC, Waters) coupled with nano-electrospray tandem mass spectrometry on a Q-TOF Ultima API mass spectrometer (Micromass/Waters) at a flow rate of 600 nl/min. The gradient was 0–50% acetonitrile in 0.1 % formic acid over 45 min. The instrument was operated in MS continuum mode and the data acquisition was from *m/z* 100–3,000 at a scan rate of 1 s and an interscan delay of 0.1 s. The spectra were accumulated over about 300 scans and the multiple charged data by the mass spectrometer on the *m/z* scale were converted to the mass (molecular weight) scale using maximum entropy-based software supplied with Masslynx 4.1 software package. The processing parameters were: output mass range 6,000–20,000 Da at a "resolution" of 0.1 Da/channel; the simulated isotope pattern model was used with the spectrum blur width parameter set to 0.2 Da, the minimum intensity ratios between successive peaks were 20% (left and right). The deconvoluted spectrum was then smoothed (2 × 3 channels, Savitzky Golay smooth) and the mass centroid values obtained using 80% of the peak top and a minimum peak width at half height of 4 channels.

2.3.2. Enzymatic hydrolysis

The purified proteins were hydrolyzed with sequencing grade bovine pancreatic trypsin in 0.4 % ammonium bicarbonate (pH 8.5), for 4 h at 37 °C, at an enzyme/substrate ratio of 1:100 (w/w). The reaction was ceased by lyophilization.

2.3.3. Analysis of tryptic digests

The proteins were reduced with 5 mM DTT (Dithiothreitol) for 25 min at 56 °C and alkylated with 14 mM iodoacetamide for 30 min prior to the addition of trypsin (Promega-Sequence Grade Modified). After the trypsin addition (20 ng/μl in ambic 0.05 M), the sample was incubated for 16 h at 37 °C. To stop the reaction, formic acid 0.4% was added and the sample centrifuged at 2500 × *g* for 10 min. The pellet was discarded and the supernatant dried. The resulting peptides were separated by C18 (100 μm × 100 mm)

RP-UPLC (nanoAcquity UPLC, Waters) coupled with nano-electrospray tandem mass spectrometry on a Q-TOF Ultima API mass spectrometer (Micromass/Waters) at a flow rate of 600 nl/min. The gradient used was 0–90% acetonitrile in 0.1% formic acid over 20 min. Before performing a tandem mass spectrum, an ESI/MS mass spectrum (TOF MS mode) was acquired for each HPLC fraction over the mass range of 100–2000 *m/z*, in order to select the ion of interest, where these ions were subsequently fragmented in the collision cell (TOF MS/MS mode).

Raw data files from LC–MS/MS runs were processed using MassLynx 4.1 SCN662 software package (Waters) and analyzed using the Mascot Distiller v.2.3.2.0, 2009 (Matrix Science, Boston, MA) with SNAKES database (snakes_jun2012 was downloaded from NCBI Taxonomy) release from June 2012, using the following parameters: peptide mass tolerance of ±0.1 Da, fragment mass tolerance of ±0.1 Da, oxidation as variable modifications in methionine and trypsin as enzyme.

2.3.4. Analysis of protein sequences

Peptide sequences were aligned using the Clustal V alignment algorithm in the MegAlign package (DNASTAR Ver. 5.01). We compared the sequences of the peptides belonging to the purified isoforms, with the complete sequences of other crotalic PLA_2 previously purified by Oliveira and collaborators (Oliveira et al., 2002).

2.4. PLA_2 activity characterization

PLA_2 activity was measured using the assay described by Holzer and Mackessy (Holzer and Mackessy, 1996), adapted for 96-well plates (Ponce-Soto et al., 2002). The standard assay mixture contained 200 μl of buffer (10 mM Tris–HCl, 10 mM $CaCl_2$, 100 mM NaCl, (pH 8), 20 μl of substrate (3 mM; 4-nitro-3-octanoyloxy-benzoic acid), 20 μl of buffer or 20 μl of enzyme in a final volume of 240 μl. After the addition of venom or PLA_2 (20 μg), the mixture was incubated for up to 30 min at 37 °C, and the absorbance at 425 nm were recorded at 10 min intervals. Enzymatic activity, expressed as velocity of reaction (V_0), was calculated based on the increase in absorbance after 20 min.

The optimal pH and temperature of PLA_2s isoforms were determined by incubating the reactions mixtures in buffers (15 mM citrate, 10 mM Tris–HCl and 15 mM Glicine, all of them with 10 mM $CaCl_2$ and 100 mM NaCl) of different pH (4–6; 7–8 and 9–10, respectively) and at different temperatures (20–70 °C) in 10 mM Tris–HCl, (pH 8.0). The enzymatic activity was also tested incubating each toxin with Mg^{+2}, Zn^{+2} or Cd^{+2} (10 mM) in presence (1 mM) or absence (0 mM) of Ca^{+2} and it was compared with that obtained with Ca^{2+} 10 mM.

All assays were done in triplicate and the absorbances at 425 nm were measured with a VersaMax 190 multiwell plate reader (Molecular Devices, S., CA).

2.5. Chick biventer cervicis muscle preparation

Animals were anesthetized with chloral hydrate (3 mg/kg) and sacrificed by exsanguination. The biventer cervicis muscles were removed and mounted under a tension of 0.5 g, in a 5 ml organ bath at 37 °C (Automatic organ multiple-bath LE01 Letica Scientific Instruments. Barcelona, Spain), containing aerated (95% O_2–5% CO_2) Krebs solution (pH 7.5) of the following composition: 118.7 mM NaCl, 4.7 mM KCl, 1.88 mM $CaCl_2$, 1.17 mM KH_2PO_4, 1.17 mM $MgSO_4$, 25.0 mM $NaHCO_3$ and 11.65 mM glucose. Contracture to exogenously applied acetylcholine (Ach, 55 and 110 μM) and KCl (20 mM) were obtained in the absence of field stimulation, prior to the addition of a single dose (10 μg) of each PLA_2s. A bipolar platinum ring electrode was placed around the tendon in which runs the nerve trunk supplying the muscle. Indirect stimulation was performed with a (MAIN BOX LE 12,404 Panlab s.l. Powerlab AD Instruments Barcelona, Spain) stimulator (0.1 Hz, 0.2 ms, 5 V). Muscle contractions and contractures were isometrically recorded via a force–displacement transducer (Model MLT0201 Force transducer 5 mg–25 g Panlab s.l. AD Instruments Pty. Ltd., Spain) connected to a PowerLab/4SP (OUAD Bridge AD Instruments, Barcelona, Spain). At the end of the experiment, muscles were washed with Krebs solution, and muscle contraction was again tested with the addition of exogenous ACh or KCl. Experiments were carried out in triplicate.

2.6. Lethality

The lethal activity of each PLA_2 isoform was tested. For this, groups of six mice were injected i.p. with 0.1 ml of solution containing 0.1–20 μg of toxin. Control mice received 0.1 ml of phosphate buffered saline solution (pH 7.2). Deaths were recorded for 48 h; Lethal Dose 50 (LD_{50}) and its confidence limits were estimated using the Spearman-Karber method (Acosta et al., 2003). LD_{50} was expressed as micrograms of toxin per mouse (18–20 g) required to kill 50 percent of the population of tested animals.

2.7. Myotoxic activity

Groups of four Swiss mice (18–20 g) received an intramuscular (i.m.) injection with 1 or 10 μg of PLA_2s samples (50 μl) in the right gastrocnemius. A control group received 50 μl of PBS. At different intervals (0.5; 1; 3; 6; 9 and 24 h), blood was collected from the tail into heparinized capillary tubes, and the plasma creatine kinase (CK; EC 2.7.3.2) activity was determined by a kinetic assay (Laborlab-CK-NAC UV). Activity was expressed in U/l, one unit defined as the phosphorylation of 1 mmol of creatine/min at 25 °C.

In order to assess the damage caused by the isoforms, the gastrocnemius muscle of 3 animals from each group were processed for ultra-structural examination and histological observations were developed with optical and transmission electron microscopy. Samples were fixed and processed following the classical histopathological technique, and were stained with hematoxylin and eosin (H&E). For electron microscopy observations, the tissue was cut into small pieces (1 × 1 mm), dissected away and fixed with 2% (v/v) glutaraldehyde in buffer phosphate at 4 °C for 2 h, after fixation the tissue was washed and soaked in phosphate buffer and sent to the Electron Microscopy Central Service of the Veterinary Faculty, National University of La Plata. The tissue was then post-fixed in 1% (w/v) osmium tetroxide, and embedded in Araldite. Thin sections (about 1 mm) were stained with toluidine blue and inspected by light microscopy in order to select fields. Ultrathin sections were mounted on 200-mesh copper grids, stained with uranyl acetate and lead citrate, and examined in a JEM-1200 EX transmission electron microscope at 80 kV.

2.8. Antitoxin production

2.8.1. Immunization process

Mice were immunized by successive intramuscular and subcutaneous inoculations with 1 to 10 μg of PLA_2 isoforms per mouse ($n = 5$ per grup), in order to obtain anti-P9a(*Cdt*-PLA_2) IgG and anti-P10a(*Cdt*-PLA_2) IgG. The first injections included Freund's complete adjuvant (Sigma) in a 1:1 ratio. The subsequent boosters were given in the same way, but using Freund's incomplete adjuvant with the toxin dissolved in PBS. Control animals were inoculated only with adjuvant. The full development of the immunization process lasted two months and every two weeks the

antibodies level in the sera was monitored by ELISA. Blood samples were collected from the mouse-tail and stored at 4 °C. The sera were subsequently separated by centrifugation and aliquots were stored at −70 °C (see Table 1, Supplementary data). IgG antibodies were purified by affinity chromatography (HiTrap Protein G HP 1 ml, Amersham Biosciences, Sweden) in a FPLC System, according to the manufacturer's instructions to obtain IgG fraction. Reactivity and specificity of anti-P9a(*Cdt*-PLA_2) IgG and anti-P10a(*Cdt*-PLA_2) IgG were tested by ELISA and dot blotting (Fusco et al., 2015; Kaiser and Middlebrook, 1988; Rodríguez et al., 2009; Rodríguez et al., 2012).

2.8.2. ELISA and dot blotting tests

Briefly, microtiter plates (96 wells) were coated with 100 μL of PLA_2 isoforms (5 μg/well) in PBS for 1 h at 37 °C. The plates were washed and processed as described by (Rodríguez et al., 2012). Absorbance was read at 490 nm with a Multiskan® EX (Thermo Scientific, USA) multiwell plate reader.

In order to provide highly specific results a dot blot test was performed. All PLA_2 isoforms were diluted in a 20 mM Tris 500 mM NaCl buffer (TBS), pH 7.2; and 5 μg were pipetted into each dot in a vertical row of a nitrocellulose strip (Bio-Rad, USA). The membranes were dried at room temperature for two hours. After that, the strips were washed once with TBS containing 0.1% (v/v) Tween 20 (TBS-Tween 20) and blocked with bovine serum albumin (1% in TBS-Tween 20) for one hour at 37 °C, on plates on a shaking platform. Then, strips were washed once with TBS-Tween 20 and immediately incubated with the corresponding antitoxin for one hour at 37 °C. Bound antibodies were detected with goat anti-mouse IgG peroxidase conjugate (Sigma, USA; 1:1000 in TBS) incubating the strips in the same conditions. Finally, blots were washed, developed with 4-chloro-1-naphthol (Sigma, USA; 0.03% in 0.05 M Tris–HCl, pH 7.6, containing 0.03% H_2O_2/OPD) and documented. Mice pre-immune serum was employed as negative control.

*2.8.3. Histopathological analysis of muscles from animals immunized with P9a(*Cdt-*PLA_2*) and P10a(*Cdt-*PLA_2*).*

Ten days after the end of the immunization protocol, the gastrocnemius muscle was extracted from its anatomical compartment and samples were taken from the middle third of the muscle to evaluate the ability of tissue regeneration. Tissue blocks of muscle were fixed in 10% formalin, dehydrated in alcohol and embedded in paraffin wax. Sections of 5 μm-thick were cut and stained with hematoxylin and eosin (H&E) or Gomory trichrome stain and examined with a Leitz light microscope.

2.9. Statistical analysis

The results are reported as the mean ± SD. The significance of differences between the means was assessed by ANOVA followed by Dunnett's test when various experimental groups were compared with the control group. A value of $p < 0.05$, indicated significance.

3. Results

3.1. Toxins purification

Four PLA_2s isoenzymes were purified from *C.d.t.* venom by a two-step procedure on molecular exclusion and reverse-phase chromatography columns. The elution profile of *C.d.t.* venom on Sephadex G75 showed three main peaks, named Cdt I, Cdt II, and Cdt III (Fig. 1A). Cdt II peak contained several proteins, as shown in the Fig. 1A insert (line 3), and it was the main eluted fraction. This fraction was further fractionated on a HPLC reverse-phase chromatographic column and it resolved fifteen peaks. Fractions 5, 6, 7 and 8 showed PLA_2 activity, were collected and designated as P9a(*Cdt*-PLA_2), P9b(*Cdt*-PLA_2), P10a(*Cdt*-PLA_2) and P10b(*Cdt*-PLA_2) respectively (Fig. 1B). The homogeneity of these PLA_2s was demonstrated by Tricine–SDS-PAGE (Fig. 1B insert) showing a single band and a relative molecular mass of ~14.4 kDa under non-reducing condition and in presence of DTT (1 M). Subsequently the homogeneity of the purification was shown by ESI–Q TOF mass spectrometry (see Supplementary data; Fig. 1). The purification process yielded around 1.25 mg of each of the three most abundant PLA_2s from 25 mg of whole venom.

3.2. Molecular mass and protein sequence determination of PLA_2s

ESI-Q-TOF mass spectrometry analysis confirmed the homogeneity of P9a(*Cdt*-PLA_2), P9b(*Cdt*-PLA_2), P10a(*Cdt*-PLA_2) and P10b

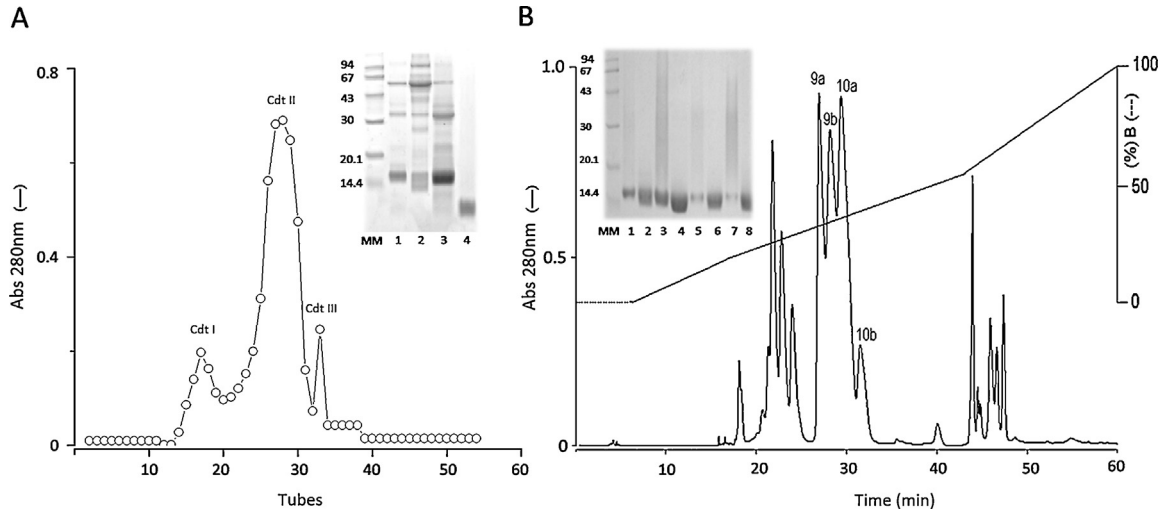

Fig. 1. (A) Molecular exclusion chromatography of *C.d.t.* venom from Argentina on Sephadex G-75. The main fractions obtained are identified as Cdt I–III. Insert: 1. *C.d.t.* venom; 2. Cdt I; 3. Cdt II; 4. Cdt III. (B) Chromatographic profile of the fractions P9a(*Cdt*-PLA_2), P9b(*Cdt*-PLA_2), P10a(*Cdt*-PLA_2) and P10b(*Cdt*-PLA_2) purification obtained in reverse phase-HPLC from Sephadex G75 peak II (Cdt II). Insert: Tricine–SDS PAGE of P9a(*Cdt*-PLA_2), P9b(*Cdt*-PLA_2), P10a(*Cdt*-PLA_2) and P10b(*Cdt*-PLA_2) isoforms in native (line 1, 3, 5, 7) and reduced conditions (line 2,4,6,8) respectively. MM, molecular mass markers ($\times 10^{-3}$ Da; markers: phosphorylase b-94, albumin-67, ovalbumin-45, carbonic anhydrase-30, trypsin inhibitor-20.1, α-lactalbumin-14.4).

(*Cdt*-PLA$_2$) and determined the molecular mass of them in 14,193.8340 Da; 14,134.9102 Da; 14,242.6289 Da; and 14,183.8730 Da, respectively (Fig. 1. Supplementary data)

The deduced partial sequences of all PLA$_2$ isoforms show that they share a high degree of identity. A comparative analysis among them was carried out using DNAStar software (v5.1); it reveled that they are not so different from others previously sequenced by 3and collaborators (Oliveira et al., 2002). These tests allow us to verify that all isoforms are different but share a high grade of identity. We only found differences between P9a(*Cdt*-PLA$_2$) and P10a(*Cdt*-PLA$_2$) at positions 105 and 106, however, their strong different chromatographic retention times suggest that they may differ in regions not yet sequenced (see Supplementary data, Fig. 2).

3.3. Activity measurements of PLA$_2$ isoforms

The enzymatic activity of PLA$_2$ isoforms, was studied using the synthetic chromogenic substrate 4-nitro-3-(octanoyloxy) benzoic acid. Fig. 2 shows the enzymatic activity of *C.d.t.* venom (1 mg/ml) and PLA$_2$ isoforms (1 mg/ml). It can be seen that the activity of the former is about 50–60%lower than those exhibited by the purified isoforms which are not significantly different among them.

On the other hand, all PLA$_2$ isoform had an optimum pH 8 and the maximum enzymatic activity was observed between 35 and 40 °C, which was lost at temperatures above of 60 °C. Under optimal conditions, all isoforms mainly showed a Michaelian behavior and a strict dependence of Ca^{+2} (10 mM and 1 mM) for full enzymatic activity (100% of activity). Pre-incubations of Mg^{+2}, Zn^{+2} or Cd^{+2} (10 mM) with PLA$_2$s isoforms in absence of Ca^{+2} (0 mM) had a significant reduction ($p < 0.05$) over the enzymatic activity compared with that obtained with Ca^{2+} 10 mM.

3.4. Neurotoxic activity

To assess PLA$_2$s neurotoxic activity, we used young chick biventercervicis nerve–muscle preparation as an experimentation model. Ten micrograms of PLA$_2$s were tested on indirectly stimulated preparations. The isoforms ($n = 3$, each) elicited an evident neurotoxic "ex vivo" effect, with a slow and progressive decrease in the twitch response to nerve stimulations (Fig. 3). *C.d.t.* whole venom was also included in this study and, as expected, it exhibited the most intense neuromucscular blockade. Analyzing chicken biventer cervicis preparations exposed to the action of PLA$_2$ isoforms, we observed that P9a(*Cdt*-PLA$_2$) and P10a(*Cdt*-PLA$_2$) produce lower effect than the other two and notably, the former is much more less neurotoxic that the others. During the first 60–70 min of the experiment P9a(*Cdt*-PLA$_2$) and control were indistinguishable, and at the end, this isoform only blockade 20% of the muscular contraction. On the other hand, P10a(*Cdt*-PLA$_2$) had a slightly different behavior, in the first 40 min caused a blockade of almost 20% and then remained constant with a slight drop in muscle contraction (Fig. 3). The other two isoforms, P9b (*Cdt*-PLA$_2$) and P10b(*Cdt*-PLA$_2$), reaching a blockade over 40%. At the tested concentration, all isoforms did not show any significant interference ($p > 0.05$) over the contracture produce by Ach (55 and 110 μM), on the other hand, the contracture produce by KCl (20 mM) was decreased.

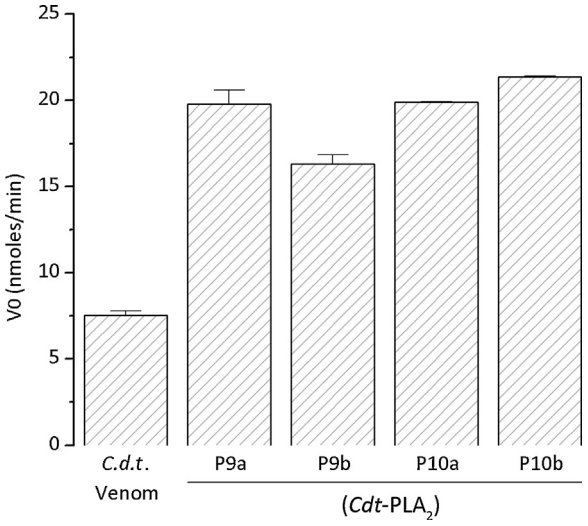

Fig. 2. Enzimatic activity characterization of P9a(*Cdt*-PLA$_2$), P9b(*Cdt*-PLA$_2$), P10a (*Cdt*-PLA$_2$) and P10b(*Cdt*-PLA$_2$) isoforms of *C.d.t.* venom. The catalytic activity was measured using the purified enzymes and 4-nitro-3-octanoyloxybenzoic acid substrate in 10 mM Tris–HCl, 10 mM $CaCl_2$, 100 mM NaCl buffer (pH 8). The results of all experiments are the mean ± SD of three determinations ($p < 0.05$).

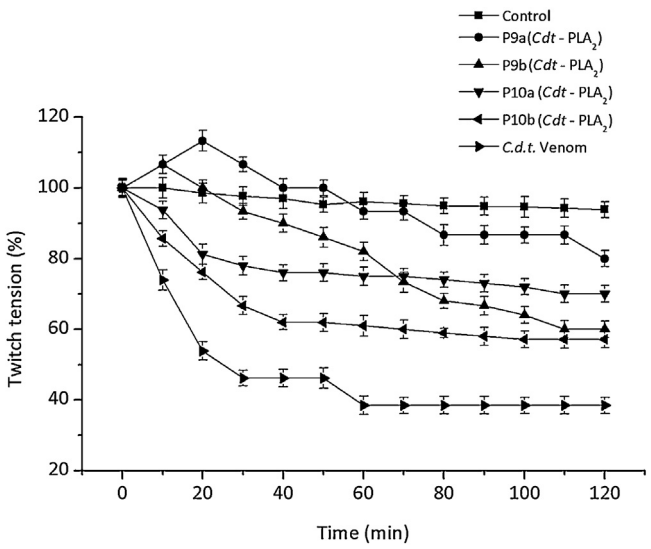

Fig. 3. Neuromuscular blockade of chick biventercervicis preparations incubated at 37 °C with whole venoms and PLA$_2$s isoforms (10 μg). The points are the mean ± SD of three experiments.

3.5. Lethality

Groups of six male Swiss white mice were injected i.p. with different doses of isoforms and the death survival ratio determined after 48 h. The LD_{50} value was calculated by probit analysis at 95% confidence. It conclusively revels and quantifies the differences of pharmacological activity observed in previous trials. We obtained 14 ± 1.5 μg, 6 ± 0.4 μg, 12 ± 0.9 μg, 4 ± 1.1 μg for P9a(*Cdt*-PLA$_2$), P9b(*Cdt*-PLA$_2$), P10a(*Cdt*-PLA$_2$) and P10b(*Cdt*-PLA$_2$) respectively. Statistical analysis revealed no significant difference between P9a (*Cdt*-PLA$_2$) and P10a(*Cdt*-PLA$_2$) or P9b(*Cdt*-PLA$_2$) and P10b(*Cdt*-PLA$_2$). However the first and third or second and fourth possess significant differences ($p < 0.05$). All isoforms showed to be less lethal than the whole venom (LD_{50} 2 ug / mouse) (Fusco et al., 2015) and P9a(*Cdt*-PLA$_2$) exhibited the highest dose.

3.6. Myotoxicity

Taking into account the values obtained in the neurotoxicity and lethality trials, we decided to target P9a(*Cdt*-PLA$_2$) and P10a (*Cdt*-PLA$_2$) as possible isoforms to be used in the production of rattlesnake antitoxins.

Fig. 4A and B show that both PLA$_2$ isoforms induced a conspicuous myotoxic effect, evidenced by a dose-dependent elevation of plasma CK. P10a(*Cdt*-PLA$_2$) showed the highest activity

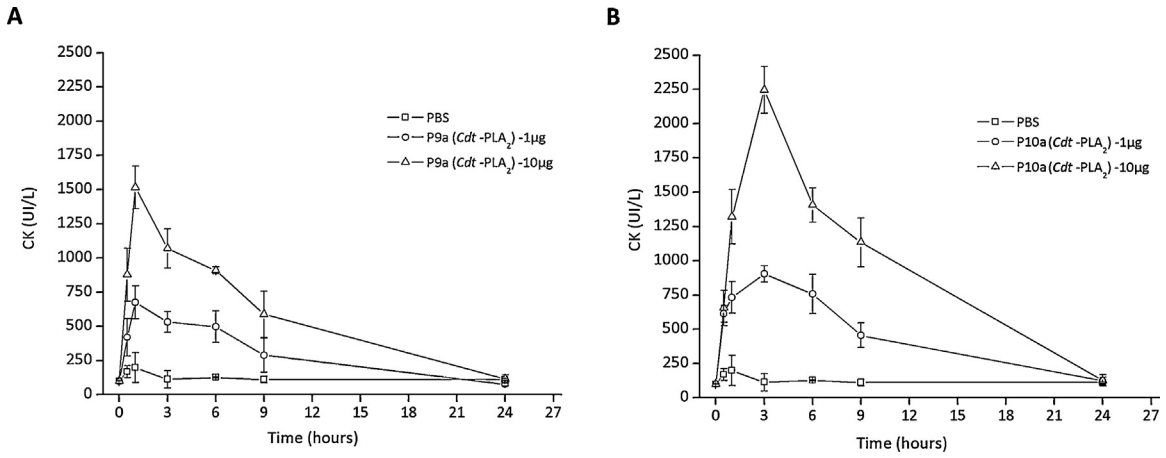

Fig. 4. Myotoxic activity of PLA_2s isoforms. (A) Time course (24 h) of Plasmatic CK release produced by 1 or 10 μg of P9a(*Cdt*-PLA_2) or P10a(*Cdt*-PLA_2) (B). The results of all experiments are the mean ± SD of three determinations ($p < 0.05$).

and it was found 3 h after injection of 1 or 10 μg/mouse of toxin. On the other hand, P9a(*Cdt*-PLA_2) showed an earlier and less intense plasma CK release. These differences could be observed only when 10 μg of toxin were injected, as they showed a quite similar behavior with 1 μg. Despite this, the time-course analysis evidenced a rapid activity, which reached a maximum increase 1–3 h after i.m. injection, and returned to normal by 24 h. These results slightly differ with the plasmatic CK kinetics release exhibited by the whole venom as described earlier (Fusco et al., 2015). It showed a maximum release of the enzyme at 6 h after

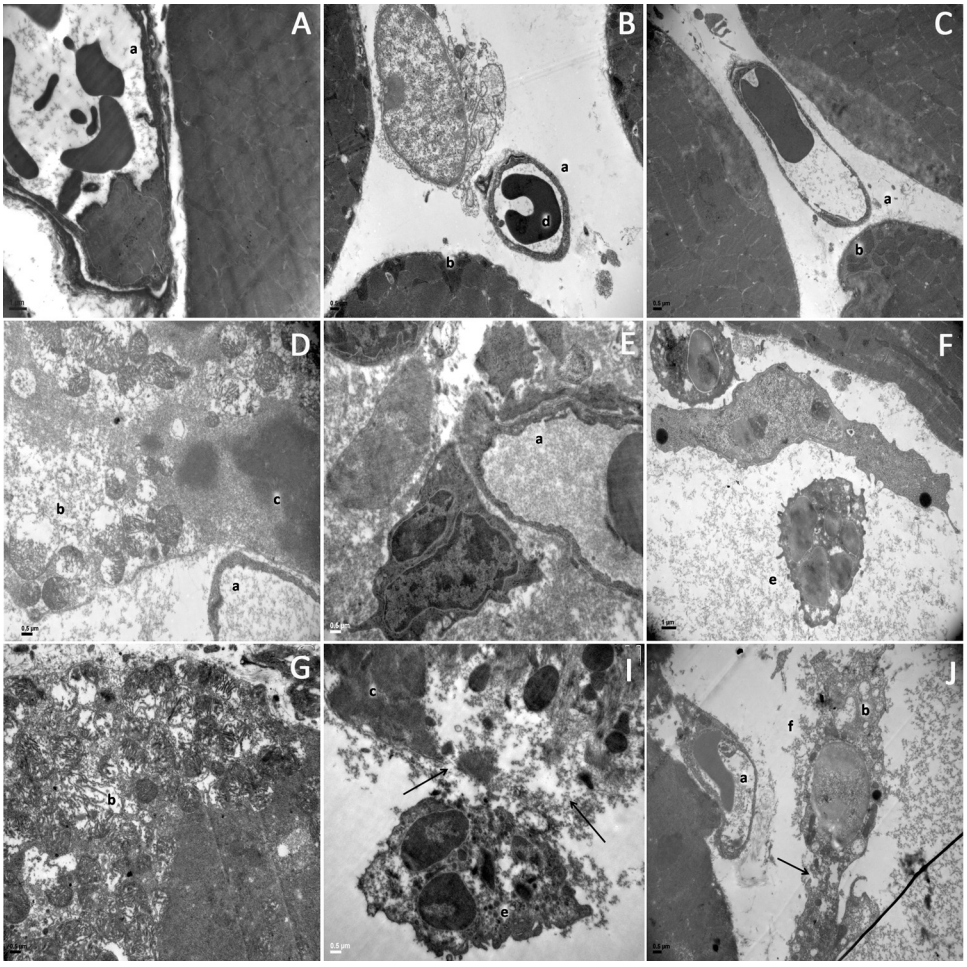

Fig. 5. Effects of PLA_2 myotoxin from *C.d.t.* venom on murine skeletal muscle. Electron micrographs of the transversal section of gastrocnemius muscle fiber showing the ultrastructural appearance of the normal and pathologic changes. (A–C). Controls muscles. (D–F) Muscles treated with P9a(*Cdt*-PLA_2) or P10a(*Cdt*-PLA_2) (G–I). 10 μg of PLA_2 were inoculated (IM) and 6 h after samples were taken and processed for transmission electron microscopy as described in Section 2. Note the intensity of the damage produced by P10a(*Cdt*-PLA_2) (lower panels) as compared to control (upper panels) or P9a(*Cdt*-PLA_2) (intermediate panels) (a) blood vessel, (b) mitochondria, (c) prominent hypercontraction of myofilaments, (d) red blood cell, (e) neutrophil, (f) macrophage. →: rupture of plasmatic membranes.

injection compared to these earlier peaks displayed by the isoforms. These differences are probably due to the fact that in the crude venom PLA_2s isoforms are complexed with crotapotin. (see Supplementary data 3).

In order to evaluate the extent of damage, gastrocnemius muscle samples exposed to the action of toxins, at different times and concentrations (1 and 10 μg of toxins; 1, 3, 6 and 24 h.), were processed for a classical histopathological study (H&E). We did not find abnormal changes in animals treated with 1 μg of toxins, on the other hand, abundant interfibrillar material and destroyed muscle fibers could be observed in mice treated with 10 μg of both toxins. However, we did not find any particular structural feature in the damage caused by each isoform. In order to further analyze these morphological changes, we studied those samples by transmission electron microscope and we noted clear abnormal alterations only in those animals treated with 10 μg and 6 h of exposure. We detected a characteristic myotoxic injury as hypercontraction of myofilaments, mitochondrial swelling, and the formation of flocculent densities. In addition to all the above effects, P10a(*Cdt*-PLA_2) produced more intense cellular damage including rupture of mitochondrial membranes or disruption of plasmatic membranes. Taking together, all the patterns observed led us to think that the swelling provokes the rupture of plasma and organelle membranes and dissolution of organized structure, typical morphological changes consistent with coagulative necrosis. In control samples a highly conserved structure of muscle fibers, mitochondria, and basal membranes can be observed (Fig. 5).

3.7. Antitoxins production

The reactivity determined by ELISA of anti-P9a(*Cdt*-PLA_2) IgG and anti-P10a (*Cdt*-PLA_2) IgG against their respective toxins is shown in Fig. 6A. Absorbance values show great reactivity of the antibodies produced, and therefore, good immunogenicity of the isolated toxins. As it can be noticed on panel B (Fig. 6) there is a high cross-reactivity between antibodies and all the toxins purified (P9a(*Cdt*-PLA_2), P9b(*Cdt*-PLA_2), P10a(*Cdt*-PLA_2) and P10b(*Cdt*-PLA_2)), since that strong spots were obtained in each case in the dot-blotting test.

In order to assess the feasibility of using these toxins in the rattlesnake antivenom production process, we inoculated the PLA_2 isoforms in the mice gastrocnemius muscle, according to an immunization schedule (1–10 μg; see Table 1, Supplementary data). We next evaluate the damage produced and the muscular regeneration developed. We divided the analysis in two muscular areas: central and peripheral. The central muscle area of animals treated with both toxins is characterized by the presence of large extracellular lipid vacuoles (very variable dimensions), typical of the adjuvant injection (Fig. 7A, B, E and F). Both myotoxic PLA_2 caused damage to muscle fibers reducing their number, however, during the immunization process, P10a(*Cdt*-PLA_2) showed more intense toxic effects than P9a(*Cdt*-PLA_2) (see Table 1). Equally, among the muscle fibers, clear evidence of muscle regeneration (→ row of nuclei lined up) and presence of blood capillaries (*) can be observed in those animals treated with P9a(*Cdt*-PLA_2)(Fig. 7B). In the peripheral region it is remarkable the increased presence of normal and regenerated muscle fibers and the absence of large myonecrotic areas (Fig. 7C and D). On the other hand, fibrosis, reveled with Gomori trichrome stain, is present in both regions in muescles treated with P10a(*Cdt*-PLA_2) (Fig. 7F and G) with the existence of only few fibers in regeneration (Fig. 7H). Control animals retained normal appearance and it was detected only the presence of adjuvant (not shown).

4. Discussion

Snakebite envenoming constitutes a highly relevant public health issue on a global basis and its adequate treatment is critically dependent on the ability of antivenoms to reverse venom-induced neurotoxicity, coagulopathy, myotoxicity, hypotensive shock and other signs of systemic. On the other hand, PLA_2s are among the most abundant components of snake venoms, and particularly in crotalic venoms, crotoxin accounts for 50% of the dry venom (Habermann and Breithaupt, 1978; Toyama et al., 2003). Although crotoxin from *C.d.t.* venom has been extensively studied, little is known about isoforms composition and biochemistry in order to use them as inmunogen in the process of antitoxins production.

In this paper, we isolated and characterized four PLA_2 isoforms from *C.d.t.* venom designated as P9a(*Cdt*-PLA_2), P9b(*Cdt*-PLA_2), P10a(*Cdt*-PLA_2) and P10b(*Cdt*-PLA_2). The purification protocol used was appropriated to yield four pure PLA_2 isoforms from the whole venom of *C.d.t.* from Argentina. Oliveira and collaborators using similar chromatographic steps obtained three PLA_2 isoforms, called F15, F16 and F17, from *C.d.t.* from Brazil (Boldrini-Franca

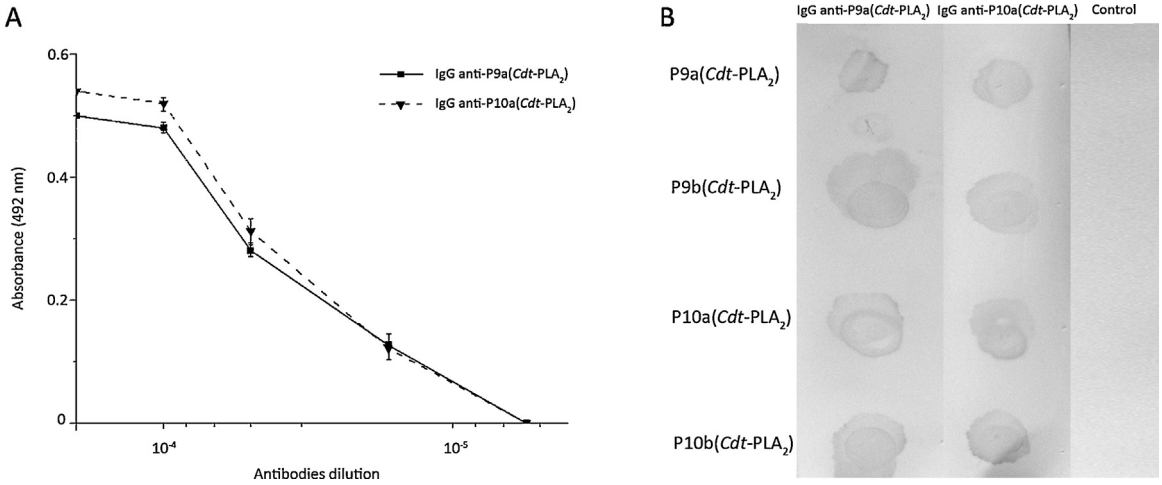

Fig. 6. (A) ELISA reactivity of anti-P9a(*Cdt*-PLA_2) IgG and anti-P10a(*Cdt*-PLA_2) IgG with PLA_2 isoforms. The plates were coated with antigen (5 μg/well) then incubated with antibodies at the dilutions indicated and finally with an appropriate IgG–peroxidase conjugate and substrate (OPD). The resulting absorbances were read at 492 nm and each point is the mean ± SD of four determinations. (B) Dot blot analysis showing the reactivity and cross reactivity of anti-P9a(*Cdt*-PLA_2) IgG and anti-P10a(*Cdt*-PLA_2) IgG with PLA_2s isoforms. Control blots were carried out in the same conditions with PBS and did not show any spots.

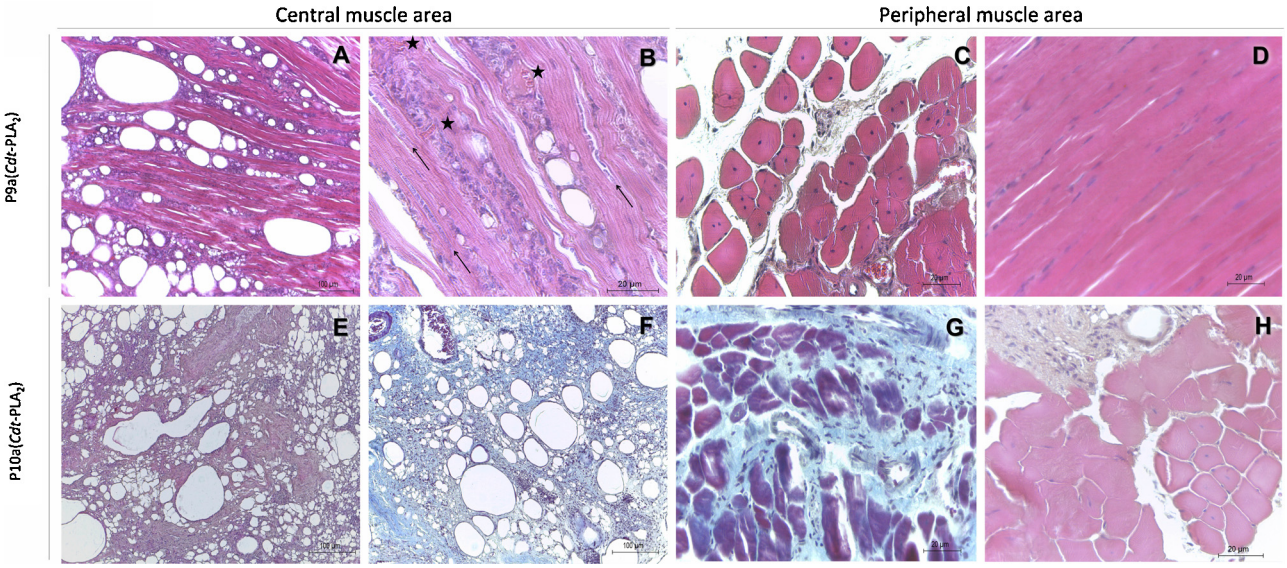

Fig. 7. Longitudinal and transversal sections of regenerative tissue and morphological changes induced in muscles from mice immunized with P9a(*Cdt*-PLA_2) and P10a(*Cdt*-PLA_2). Animals were immunized with isoforms according to the protocols described in Section 2. (A–E and H) Panels show muscles stained with H&E. Central and peripheral muscle areas show the changes induced by the inoculation of PLA_2 isoforms in the immunization process. (F and G) Fibrosis induced by P10a(*Cdt*-PLA_2) reveled by Gomori Trichrome staining. The presence of blood vessels is shown with stars (*) and the classical features of regenerating fibers with centrally located nuclei are shown with arrows (→).

Table 1
Morphological changes induced by PLA_2 isoforms after the immunization process.

	Central muscle area		Peripheral muscle area	
Cdt-PLA_2	P9a	P10a	P9a	P10a
Fibrosis	–	++	–	++
Normal muscle fibers (NMF)	+	–	+++	–
Muscle regeneration fibers (MRF)	++	–	+	+

–: Non observed, +: scare, ++: moderate, +++: abundant.

et al., 2010; Oliveira et al., 2002). This is in concordance with previous studies reported by Faure and others, who informed that crotoxin has been shown to be a mixture of isoforms with different biochemical properties (Boldrini-Franca et al., 2010; Faure et al., 1993, 1994). The chromatographic profile obtained showed that the relative abundance of each isoform is very similar, except for P10b(*Cdt*-PLA_2) which is clearly in fewer amounts.

Many works focus on the structural variability of isoforms present in *C.d.t.* venoms (Oliveira et al., 2002) or other subspecies phylogenetically separated (Ponce-Soto et al., 2007a,b; Romero-Vargas et al., 2010) and thereby explain variations in their respective pharmacological activities, in this regard a comparative analysis were carried out with DNA Star MegAlig Software (Ver. 5.01), and it showed that all isoforms have a high level of identity between them, and among other crotalic PLA_2s. Given the lack of complete sequences, we cannot quantify the identity percent of these isoforms with other of *Crotalus* gender; however, since there are no appreciable differences in the active site and the calcium binding loop regions we assume similar PLA_2 activities. In order to clarify that, we investigated the enzymatic activity of all isoforms and found that possess similar catalytic activities. Breithaupt reported that venom PLA_2 shows classic Michaelis–Menten behavior against micellar substrates (Breithaupt, 1976). However, in this work we observed that the highest enzymatic activity of PLA_2s, against a non-micellar substrate, occurs at pH 7–8 and 37–40 °C, and, these enzymes exhibit activity even at 60 °C, like other PLA_2, these isoforms are relatively resistant to heat (Damico et al., 2005; Huancahuire-Vega et al., 2011; Kini, 2003). These physicochemical properties reveal that these molecules have stable structures, which is highly desirable in order to use them as immunogens.

Since that a large amount of toxins is inoculated in animals that produce antitoxins, we made a tightly characterization of the main toxicological properties of these PLA_2 isoforms: neurotoxic, myotoxic and lethal activities.

It is widely known that the most important property exhibited by crotalic PLA_2s is neurotoxicity. All isoforms isolated in this work exhibited *in vitro* neuromuscular pre-synaptic blocking activity in chick nerve-muscle preparations. However, they showed differences on their neurotoxic effect, probably due to changes in the amino acid composition of these isoforms, around the region responsible for the neurotoxic effect in presynaptic neurotoxins (residues 80–110), which is not a conserved sequence (Kini and Iwanaga, 1986a). P9a(*Cdt*-PLA_2) or P10a(*Cdt*-PLA_2) did not show signs of interference with the muscle contractures produced by the addition of exogenous Ach, however, both isoforms produced a slide reduction on the contracture to exogenous KCl. This effect was expected since P9a(*Cdt*-PLA_2) and P10a(*Cdt*-PLA_2) produce significant myotoxicity at the same dose (see below). Altogether, the results indicate that these isoforms would not have direct action on nicotinic receptors on muscle fibers. Thus, these observations strongly suggest that the neuromuscular blockade produced by P9a(*Cdt*-PLA_2) or P10a(*Cdt*-PLA_2) isoforms was mediated primarily by a presynaptic action and it is in agreement with other PLA_2 purified from *C. d. terrificus* venom from Brazil (Toyama et al., 2003).

Regarding the neurotoxicity and according with the results described above, P9a(*Cdt*-PLA_2) or P10a(*Cdt*-PLA_2) showed to be less lethal than the others, displaying a LD_{50} 6 and 7-fold more potent than that exhibited by the whole venom, respectively. Given these trials, both isoforms are very good candidates to be used as immunogens; however, other aspects were analyzed to elucidate their organic systemic impact.

It is known that Crotoxin or crotalic PLA_2s produce local and systemic skeletal muscle necrosis (Gutierrez et al., 2008; Salvini et al., 2001) and this represent a serious complication in animals exposed to long immunization protocols in the antivenom production process. In that sense we found that P10a(*Cdt*-PLA_2) induced increments in plasma CK ~1.5 times greater than P9a(*Cdt*-PLA_2) 1–3 h after the toxin injection. It is believed that myotoxic PLA_2 affect directly the plasma membrane integrity of muscle cells, causing several degenerative events and irreversible cell injures (Andriao-Escarso et al., 2000; Costa et al., 2008; Gutierrez et al., 2008; Kini and Iwanaga, 1986b), and recently, some aspect of the mechanisms involved were clarified performing lipidomic studies (Fernandez et al., 2013). In this work we have shown that the purified isoforms produce characteristic ultrastructural damage, previously described by Gutierrez and collaborators, but in this regard we used them to further characterize their intrinsic toxicity and observe that P9a(*Cdt*-PLA_2) was less toxic than P10a(*Cdt*-PLA_2) (Gutierrez and Ownby, 2003).

Myotoxicity and neurotoxicity are two properties of crotalic PLA_2 that cannot be avoided, but compared with the action of CTX or the whole venom these pharmacological activities are much more reduced. Taking advantage of this, we recently designed alternative immunization plans to partially replace the use of whole venom with crotalic PLA_2s in the rattlesnake antivenom production process (Fusco et al., 2014).

Although we have saved time and reduced the myotoxic injury to improve animal welfare, it is well known that PLA_2 fraction still has toxic effect depending on their toxicological nature or its primary structure. In this sense, the existence of multiple isoforms present in the venom creates the possibility of choosing the least toxic to be used as immunogen. Moreover, a good immunogen not only requires being of low toxicity or even better nontoxic, in addition, antibodies generated against it, should cross-react with other isoforms equally present in the venom (Beghini et al., 2005; Choumet et al., 1991; Rodríguez et al., 2012; Stabeli et al., 2005). To check this, we inoculated the purified isoforms in mice and easily produced anti-P9a(*Cdt*-PLA_2) IgG and anti-P10a (*Cdt*-PLA_2) IgG demonstrating their immunogenicity and their capacity to cross-react with the rest of PLA_2 isoforms. Although we have not demonstrated their neutralizing capacity, our previous experience and the value of the titters obtained, lead us to think that these antibodies are similar to those obtained previously in our laboratory (Rodríguez et al., 2006; Rodríguez et al., 2009).

Focusing on the differential ability of these toxins in producing damage in target organs, histological evidence obtained clearly demonstrated that P9a(*Cdt*-PLA_2) is much less toxic than P10a(*Cdt*-PLA_2). Direct inoculation of toxins in the central area of the muscle produced a large myonecrosis that is very evident within a few days after injection and this direct action can cause thrombosis and ischemia (Gutierrez et al., 2008; Moreira et al., 2008). Necrosis is usually followed by regeneration of fibers over the following days, a process that starts in the vicinity of the undamaged muscle fibers and requires the presence of functional blood vessels unaffected. These latter are important in providing nutrients and macrophages, which phagocyte cellular debris and then synthesize the necessary fibers for tissue reconstruction (Charrin et al., 2013; Teibler et al., 2001; Teixeira et al., 2009). It is believed that successful muscle regeneration originates from satellite cells (myoblasts) that posses differentiation and migration capacity; these latter initially form a multinucleate tubular structures described as myotubes an then the fusion of various myotubes originates a single mature muscle fiber. All these structures compatible with muscle regeneration were found in the samples injected with P9a(*Cdt*-PLA_2). In contrast, those treated with P10a (*Cdt*-PLA_2), developed an intense fibrosis; this may be possible given its greater toxicity. Since that regeneration originates in the undamaged area, the possible existence of large necrotic foci with dead satellite cells prevents muscle regeneration.

It is clear that venoms represent a huge and essentially unexplored reservoir of bioactive components (Calvete et al., 2009) that must be analyzed with the aim of finding antigens with high immunogenicity and low toxicity. Thus, in order to develop secure protocols for the production of effective antitoxins, this work highlights that P9a(*Cdt*-PLA_2) has some distinguished conditions like a good purification performance and low toxicity, what makes this isoform a good candidate to produce anti-crotalic PLA_2 IgG; therefore, it is an attractive option to be used as an immunogen, to partially replace the use of whole venom with this isoform, in the rattlesnake antivenom production process. Additionally, this study provide a deeper knowledge in the understanding of variations in antigenic constituents of venoms, since it represents a key challenge, towards the design of novel toxin-specific approaches for the immunotherapy of snake bite envenoming.

Acknowledgments

This research was financialy supported by Secretaría General de Ciencia y Técnica (SGCyT)CF01/2013-CF02/2013 Universidad Nacional del Nordeste (UNNE). The authors thank to CEPSAN, Corrientes, Argentina for providing the venom from *Crotalus durissus terrificus* species. Luciano S. Fusco is the recipient of a doctoral fellowship supported by CONICET–UNNE.

Appendix A. Supplementary data

Supplementary data associated with this article can be found, in the online version, at http://dx.doi.org/10.1016/j.toxlet.2015.06.528.

References

Acosta, O., Leiva, L.C., Peichoto, M.E., Marunak, S., Teibler, P., Rey, L., 2003. Hemorrhagic activity of the Duvernoy's gland secretion of the xenodontine colubrid *Philodryas* patagoniensis from the north-east region of Argentina. Toxicon 41, 1007–1012.

Andriao-Escarso, S.H., Soares, A.M., Rodrigues, V.M., Angulo, Y., Diaz, C., Lomonte, B., Gutierrez, J.M., Giglio, J.R., 2000. Myotoxic phospholipases A(2) in bothrops snake venoms: effect of chemical modifications on the enzymatic and pharmacological properties of bothropstoxins from *Bothrops jararacussu*. Biochimie 82, 755–763.

Beghini, D.G., da Cruz-Hofling, M.A., Randazzo-Moura, P., Rodrigues-Simioni, L., Novello, J.C., Hyslop, S., Marangoni, S., 2005. Cross-neutralization of the neurotoxicity of *Crotalus durissus terrificus* and *Bothrops jararacussu* venoms by antisera against crotoxin and phospholipase A_2 from *Crotalus durissus* cascavella venom. Toxicon 46, 604–611.

Boldrini-Franca, J., Correa-Netto, C., Silva, M.M., Rodrigues, R.S., De La Torre, P., Perez, A., Soares, A.M., Zingali, R.B., Nogueira, R.A., Rodrigues, V.M., Sanz, L., Calvete, J.J., 2010. Snake venomics and antivenomics of *Crotalus durissus* subspecies from Brazil: assessment of geographic variation and its implication on snakebite management. J. Proteomics 73, 1758–1776.

Breithaupt, H., 1976. Enzymatic characteristics of crotalus phospholipase A_2 and the crotoxin complex. Toxicon 14, 221–233.

Calvete, J.J., Sanz, L., Angulo, Y., Lomonte, B., Gutierrez, J.M., 2009. Venoms, venomics, antivenomics. FEBS Lett. 583, 1736–1743.

Charrin, S., Latil, M., Soave, S., Polesskaya, A., Chretien, F., Boucheix, C., Rubinstein, E., 2013. Normal muscle regeneration requires tight control of muscle cell fusion by tetraspanins CD9 and CD81. Nat. Commun. 4, 1674.

Choumet, V., Jiang, M.S., Specker, I., Bon, C., 1991. Immunochemical cross-reactivity of two phospholipase A_2 neurotoxins, agkistrodotoxin and crotoxin. Toxicon 29, 441–451.

Costa, T.R., Menaldo, D.L., Oliveira, C.Z., Santos-Filho, N.A., Teixeira, S.S., Nomizo, A., Fuly, A.L., Monteiro, M.C., de Souza, B.M., Palma, M.S., Stabeli, R.G., Sampaio, S.V.,

Soares, A.M., 2008. Myotoxic phospholipases A(2) isolated from *Bothrops brazili* snake venom and synthetic peptides derived from their C-terminal region: cytotoxic effect on microorganism and tumor cells. Peptides 29, 1645–1656.
Damico, D.C., Lilla, S., de Nucci, G., Ponce-Soto, L.A., Winck, F.V., Novello, J.C., Marangoni, S., 2005. Biochemical and enzymatic characterization of two basic Asp49 phospholipase A_2 isoforms from *Lachesis muta* muta (Surucucu) venom. Biochim. Biophys. Acta 1726, 75–86.
Faure, G., Harvey, A.L., Thomson, E., Saliou, B., Radvanyi, F., Bon, C., 1993. Comparison of crotoxin isoforms reveals that stability of the complex plays a major role in its pharmacological action. Eur. J. Biochem. 214, 491–496.
Faure, G., Choumet, V., Bouchier, C., Camoin, L., Guillaume, J.L., Monegier, B., Vuilhorgne, M., Bon, C., 1994. The origin of the diversity of crotoxin isoforms in the venom of *Crotalus durissus terrificus*. Eur. J. Biochem. 223, 161–164.
Fernandez, J., Lomonte, B., Sanz, L., Angulo, Y., Gutierrez, J.M., Calvete, J.J., 2010. Snake venomics of *Bothriechis nigroviridis* reveals extreme variability among palm pitviper venoms: different evolutionary solutions for the same trophic purpose. J. Proteome Res. 9, 4234–4241.
Fernandez, J., Caccin, P., Koster, G., Lomonte, B., Gutierrez, J.M., Montecucco, C., Postle, A.D., 2013. Muscle phospholipid hydrolysis by *Bothrops* asper Asp 49 and Lys 49 phospholipase a myotoxins: distinct mechanisms of action. FEBS J..
Fusco, L.S., Rodriguez, J.P., Teibler, P., Marunak, S., Acosta, O., Leiva, L., 2014. New immunization protocol to produce crotalic antivenom combining *Crotalus durissus terrificus* venom and its PLA. Biol. J. Int. Assoc. Biol. Stand..
Fusco, L.S., Rodriguez, J.P., Teibler, P., Marunak, S., Acosta, O., Leiva, L., 2015. New immunization protocol to produce crotalic antivenom combining *Crotalus durissus terrificus* venom and its PLA2. Biol. J. Int. Assoc. Biol. Stand. 43, 62–70.
Gutierrez, J.M., Ownby, C.L., 2003. Skeletal muscle degeneration induced by venom phospholipases A_2: insights into the mechanisms of local and systemic myotoxicity. Toxicon 42, 915–931.
Gutierrez, J.M., Ponce-Soto, L.A., Marangoni, S., Lomonte, B., 2008. Systemic and local myotoxicity induced by snake venom group II phospholipases A2: comparison between crotoxin, crotoxin B and a Lys49 PLA2 homologue. Toxicon 51, 80–92.
Gutierrez, J.M., 2002. Understanding snake venoms: 50 years of research in Latin America. Rev. Biol. Trop. 50, 377–394.
Habermann, E., Breithaupt, H., 1978. Mini-review. The crotoxin complex–an example of biochemical and pharmacological protein complementation. Toxicon 16, 19–30.
Hendon, R.A., Fraenkel-Conrat, H., 1971. Biological roles of the two components of crotoxin. Proc. Natl. Acad. Sci. U. S. A. 68, 1560–1563.
Hendon, R.A., Fraenkel-Conrat, H., 1976. The role of complex formation in the neurotoxicity of crotoxin components A and B. Toxicon 14, 283–289.
Hendon, R.A., Tu, A.T., 1979. The role of crotoxin subunits in tropical rattlesnake neurotoxic action. Biochim. Biophys. Acta 578, 243–252.
Holzer, M., Mackessy, S.P., 1996. An aqueous endpoint assay of snake venom phospholipase A_2. Toxicon 34, 1149–1155.
Huancahuire-Vega, S., Ponce-Soto, L.A., Martins-de-Souza, D., Marangoni, S., 2011. Biochemical and pharmacological characterization of PhTX-I a new myotoxic phospholipase A_2 isolated from *Porthidium* hyoprora snake venom. Comp. Biochem. Physiol. C Toxicol. Pharmacol. 154, 108–119.
Kaiser, I.I., Middlebrook, J.L., 1988. Preparation of a crotoxin neutralizing monoclonal antibody. Toxicon 26, 855–865.
Kini, R.M., Iwanaga, S., 1986a. Structure-function relationships of phospholipases. I: prediction of presynaptic neurotoxicity. Toxicon 24, 527–541.
Kini, R.M., Iwanaga, S., 1986b. Structure-function relationships of phospholipases. II: charge density distribution and the myotoxicity of presynaptically neurotoxic phospholipases. Toxicon 24, 895–905.
Kini, R.M., 2003. Excitement ahead: structure, function and mechanism of snake venom phospholipase A_2 enzymes. Toxicon 42, 827–840.
Marchi-Salvador, D.P., Correa, L.C., Salvador, G.H., Magro, A.J., Oliveira, C.Z., Iulek, J., Soares, A.M., Fontes, M.R., 2007. Preliminary X-ray crystallographic studies of a tetrameric phospholipase A_2 formed by two isoforms of crotoxin B from *Crotalus durissus terrificus* venom. Acta Crystallogr. Sect. F Struct. Biol. Cryst. Commun. 63, 1067–1069.
Moreira, V., Gutierrez, J.M., Soares, A.M., Zamuner, S.R., Purgatto, E., Teixeira Cde, F., 2008. Secretory phospholipases A(2) isolated from Bothrops asper and from *Crotalus durissus terrificus* snake venoms induce distinct mechanisms for biosynthesis of prostaglandins E2 and D2 and expression of cyclooxygenases. Toxicon 52, 428–439.
Oliveira, D.G., Toyama, M.H., Novello, J.C., Beriam, L.O., Marangoni, S., 2002. Structural and functional characterization of basic PLA2 isolated from *Crotalus durissus terrificus* venom. J. Protein Chem. 21, 161–168.
Ponce-Soto, L.A., Toyama, M.H., Hyslop, S., Novello, J.C., Marangoni, S., 2002. Isolation and preliminary enzymatic characterization of a novel PLA2 from *Crotalus durissus* collilineatus venom. J. Protein Chem. 21, 131–136.
Ponce-Soto, L.A., Bonfim, V.L., Rodrigues-Simioni, L., Novello, J.C., Marangoni, S., 2006. Determination of primary structure of two isoforms 6-1 and 6-2 PLA2 D49 from *Bothrops jararacussu* snake venom and neurotoxic characterization using in vitro neuromuscular preparation. Protein J. 25, 147–155.
Ponce-Soto, L.A., Baldasso, P.A., Romero-Vargas, F.F., Winck, F.V., Novello, J.C., Marangoni, S., 2007a. Biochemical, pharmacological and structural characterization of two PLA2 isoforms Cdr-12 and Cdr-13 from *Crotalus durissus* ruruima snake venom. Protein J. 26, 39–49.
Ponce-Soto, L.A., Lomonte, B., Rodrigues-Simioni, L., Novello, J.C., Marangoni, S., 2007b. Biological and structural characterization of crotoxin and new isoform of crotoxin B PLA(2) (F6a) from *Crotalus durissus* collilineatus snake venom. Protein J. 26, 221–230.
Rodríguez, J.P., De Marzi, M., Marunak, S., Malchiodi, E.L., Leiva, L.C., Acosta, O., 2006. Rabbit IgG antibodies against phospholipase A_2 from *Crotalus durissus terrificus* neutralize the lethal activity of the venom. Medicina (B Aires) 66, 512–516.
Rodríguez, J.P., De Marzi, M.C., Maruñak, S., Teibler, P., Acosta, O., Malchiodi, E.L., Leiva, L.C., 2009. IgG antibodies against phospholipase A_2 from *Crotalus durissus terrificus*: cross-reaction with venoms from *Bothrops* species from Argentina. J. Venom. Anim. Toxins Incl. Trop. Dis. 15, 460–478.
Rodríguez, J.P., Gay, C.C., Fusco, L.S., Gauna, M.C., Acosta, O.C., Leiva, L.C., 2012. Cross-neutralization of the coagulant activity of *Crotalus durissus terrificus* venom from the northeast of Argentina by bivalent bothropic antivenom. J. Venom. Anim. Toxins Incl. Trop. Dis. 18, 116–123.
Romero-Vargas, F.F., Ponce-Soto, L.A., Martins-de-Souza, D., Marangoni, S., 2010. Biological and biochemical characterization of two new PLA2 isoforms Cdc-9 and Cdc-10 from *Crotalus durissus* cumanensis snake venom. Comp. Biochem. Physiol. C Toxicol. Pharmacol. 151, 66–74.
Salvini, T.F., Amaral, A.C., Miyabara, E.H., Turri, J.A., Danella, P.M., Selistre de Araujo, H.S., 2001. Systemic skeletal muscle necrosis induced by crotoxin. Toxicon 39, 1141–1149.
Sampaio, S.C., Hyslop, S., Fontes, M.R., Prado-Franceschi, J., Zambelli, V.O., Magro, A. J., Brigatte, P., Gutierrez, V.P., Cury, Y., 2010. Crotoxin: novel activities for a classic beta-neurotoxin. Toxicon 55, 1045–1060.
Saravia, P., Rojas, E., Arce, V., Guevara, C., Lopez, J.C., Chaves, E., Velasquez, R., Rojas, G., Gutierrez, J.M., 2002. Geographic and ontogenic variability in the venom of the neotropical rattlesnake *Crotalus durissus*: pathophysiological and therapeutic implications. Rev. Biol. Trop. 50, 337–346.
Stabeli, R.G., Magalhaes, L.M., Selistre-de-Araujo, H.S., Oliveira, E.B., 2005. Antibodies to a fragment of the *Bothrops* moojenil-amino acid oxidase cross-react with snake venom components unrelated to the parent protein. Toxicon 46, 308–317.
Teibler, P., Acosta de Perez, O., Marunak, S., Sanchez Negrette, M., Ortega, H., 2001. Muscular regeneration after myonecrosis induced by *Bothrops jararacussu* snake venom from Argentina. Biocell 25, 257–264.
Teixeira, C., Cury, Y., Moreira, V., Picolo, G., Chaves, F., 2009. Inflammation induced by *Bothrops asper* venom. Toxicon 54, 67–76.
Toyama, M.H., Carneiro, E.M., Marangoni, S., Barbosa, R.L., Corso, G., Boschero, A.C., 2000. Biochemical characterization of two crotamine isoforms isolated by a single step RP-HPLC from *Crotalus durissus terrificus* (South American rattlesnake) venom and their action on insulin secretion by pancreatic islets. Biochim. Biophys. Acta 1474, 56–60.
Toyama, M.H., de Oliveira, D.G., Beriam, L.O., Novello, J.C., Rodrigues-Simioni, L., Marangoni, S., 2003. Structural, enzymatic and biological properties of new PLA (2) isoform from *Crotalus durissus terrificus* venom. Toxicon 41, 1033–1038.